An accurate *ab initio* potential energy surface and calculated spectroscopic constants for BeH_2, BeD_2, and BeHD

Hui Li and Robert J. Le Roy[a)]
Guelph-Waterloo Centre for Graduate Work in Chemistry, University of Waterloo, Waterloo, Ontario N2L 3G1, Canada

(Received 7 March 2006; accepted 17 May 2006; published online 26 July 2006)

A three-dimensional potential energy surface for the ground electronic state of BeH_2 has been determined by three-dimensional spline interpolation over 6864 symmetry-unique *ab initio* points calculated at the icMRCI/aug-cc-pV5Z level and corrected for core-electron correlation computed at the MR-ACPF/cc-pCV5Z level. Calculated spectroscopic constants of BeH_2 and BeD_2 are in excellent agreement with recent experimental results: for 11 bands of BeH_2 and 5 bands of BeD_2 the root mean square (rms) band origin discrepancies were only 0.15(±0.09) and 0.46(±0.19) cm^{-1}, respectively, and the rms relative discrepancies in the inertial rotational constants ($B_{[v]}$) were only 0.028% and 0.023%, respectively. Spectral constants for BeHD were predicted using the same potential surface. The effect of different interpolation methods on predicted potential function values and on the calculated level energies and spectroscopic constants has been examined.
 [DOI: 10.1063/1.2212933]

I. INTRODUCTION

The BeH_2 molecule has long been the subject of theoretical studies[1–10] and has often been used as a "textbook example" of *sp* hybrid orbital bonding in introductory chemistry textbooks.[11] However, it was not observed in the gas phase until the work of Bernath *et al.* in 2002.[12] Their high resolution Fourier transform infrared emission spectroscopy studies yielded band origins and rotational constants for 11 vibrational bands of BeH_2 and 5 of BeD_2.[13,14] Most previous theoretical studies had focused on the bonding behavior in this molecule and, in particular, on the $Be+H_2 \rightarrow BeH_2$ reaction along the C_{2v} symmetry axis. A noteworthy exception was the work of Martin and Lee[3] who used augmented coupled cluster [CCSD(T)] calculations to obtain accurate quartic force field parameters, which in turn were used in perturbation theory calculations to predict the equilibrium spectroscopic constants of BeH_2. However, while their bond length was in good (0.45%) agreement with experiment, the discrepancy for their anharmonic stretching frequency was 12 cm^{-1} (or 0.41%). A recent variational configuration interaction calculation of this potential energy surface by Hrenar *et al.*[9] performed using a multilevel scheme [one dimensional (1D): CCSD(T), two dimensional (2D): MP4(SDQ), and three dimensional (3D): MP2] with a cc-pCVTZ basis set did no better in this regard, yielding a stretching frequency discrepancy of 21 cm^{-1} (or 0.98%). The object of the present work was therefore to calculate an accurate potential energy surface for BeH_2 and perform accurate direct calculations of the vibration-rotation level energies to permit comprehensive comparisons with experiment.

In the following, Sec. II describes how the *ab initio* potential function values were calculated and how eigenvalues on that potential energy surface were computed. Section III then presents the resulting potential energy surface, demonstrates an improved procedure for interpolating between the calculated grid points to obtain the potential function values required for the eigenvalue calculations, presents the calculated vibrational energies and rotational constants, and compares them with experiment. Our conclusions are summarized in Sec. IV.

II. COMPUTATIONAL METHODS

A. The potential energy surface

The three-dimensional adiabatic potential energy surface for the electronic ground state of BeH_2 has been calculated using the MOLPRO package.[15] All of these calculations were first carried out using the internally contracted multireference interaction method with Langhoff and Davidson corrections (icMRCI+Q).[16] The augmented correlation-consistent polarized quintuple-zeta (aug-cc-pV5Z or AV5Z) basis set[17] was employed, resulting in a total of 287 cGTOs (contracted Gaussian-type orbitals). All reference states were taken from the natural orbitals for a state-averaged complete active space self-consistent-field (CASSCF) calculation for equally weighted 1 $^1A'$, 2 $^1A'$, and 1 $^1A''$ states. Four active electrons and six active orbitals were used, including two for the hydrogens and four for Be. The 1*s*-like core orbital of Be was fully optimized, while being constrained to be doubly occupied and excluded from the full valence active space, denoted MCSCF (4,6), where MCSCF means multiconfiguration self-consistent field. In the subsequent MRCI calculations, the reference functions were taken to be the same as those in the CASSCF active space. The total number of contracted configurations in the MRCI calculations was about 0.65×10^6. All calculations were performed in the C_s symmetry framework.

[a)]Electronic mail: leroy@uwaterloo.ca

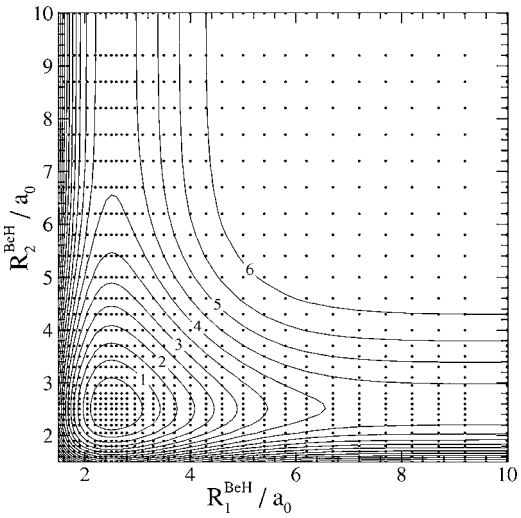

FIG. 1. Grid placement and contour plots in internal coordinates for BeH_2 at $\gamma=180°$. Contours are separated by 0.5 eV, with the zero of energy set at the potential minimum.

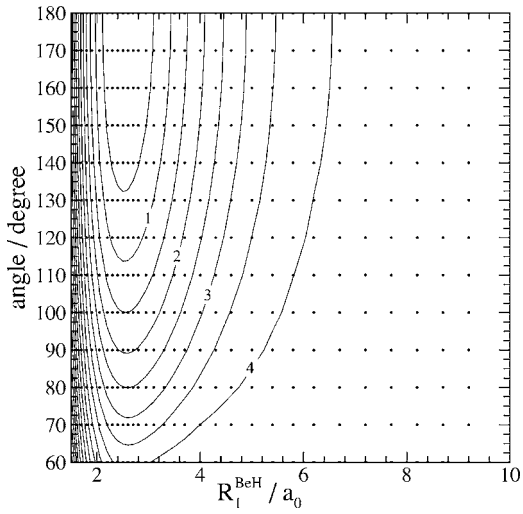

FIG. 2. Grid placement and contour plots in internal coordinates for BeH_2 at $R_2^{BeH}=2.506a_0$. Contours are separated by 0.5 eV, with the zero of energy set at the potential minimum.

To determine the core-electron correlation contribution, which is defined as the difference between the energies of a valence-only and core-plus-valence electron calculation, the energies were calculated at every point on the potential energy surface using the multireference averaged coupled pair functional (MR-ACPF) method.[18] This was done both because it is desirable to use a size-extensive method when a large numbers of electrons are correlated, and because a multireference method is more appropriate when considering a bond breaking process. A correlation-consistent polarized core-valence quintuple-zeta basis set[17] (cc-pCV5Z or CV5Z) was employed. Thus, our optimum potential energy values were obtained as

$$E^{\{\text{final}\}} = E^{\{\text{valence}\}}_{\text{AV5V}} + [E^{\{\text{valence+core}\}}_{\text{CV5Z}} - E^{\{\text{valence}\}}_{\text{CV5Z}}]. \quad (1)$$

For compactness, in the rest of the present paper calculations performed without and with the core-electron correlation contributions are called AV5Z and AV5Z+V_{core}, respectively.

A nonuniform direct-product grid in the internal coordinate system was selected for calculation of the potential energy surface. In order to obtain a particularly accurate surface, we chose a relatively dense grid in the Be–H stretching coordinates, consisting of 32 points ranging from 1.5 to $10.0a_0$, while the bending coordinate was sampled at 13 values of the enclosed angle, ranging from 60° to 180°. This gives a total of 6864 symmetry-unique points whose distribution and density are illustrated in Figs. 1 and 2. The final potential energy surface was then defined by performing three-dimensional spline interpolation over this grid of points. The potential contours and aspects of the interpolation procedure are discussed below. In some configurations where orbital mixing is strong, the MRCI and MR-ACPF calculations experienced convergence difficulties. In those situations we used the converged natural orbitals of a nearby geometry as the initial guess to improve the convergence.

To study the barrier for the reaction involving insertion of Be into H_2 on a reaction path with C_{2v} symmetry, we also calculated a two-dimensional potential energy surface at the same level of theory as before using Jacobi coordinates (R, r_{HH}, χ), in which R is the distance between the Be atom and the center of the H–H bond, and the angle between **R** and the H–H bond axis is fixed at $\chi=90°$.

B. Calculations of rovibrational energy levels

Within the Born-Oppenheimer approximation, the rovibrational Hamiltonian of a triatomic molecule in the Radau coordinate system (R_1, R_2, θ) with the total angular momentum representation in the body-fixed reference frame can be written as (in a.u.)[19–21]

$$\hat{H} = -\frac{1}{2m_1}\frac{\partial^2}{\partial R_1^2} - \frac{1}{2m_2}\frac{\partial^2}{\partial R_2^2} + \left(\frac{1}{2m_1R_1^2} + \frac{1}{2m_2R_2^2}\right)\left(\frac{-1}{\sin\theta}\frac{\partial}{\partial\theta}\sin\theta\frac{\partial}{\partial\theta} + \frac{\hat{J}_z^2}{\sin^2\theta}\right) + \frac{\hat{J}^2 - 2\hat{J}_z^2}{2m_1R_1^2} + \frac{\cot\theta}{2m_1R_1^2}[(\hat{J}_x + i\hat{J}_y) + (\hat{J}_x - i\hat{J}_y)]\hat{J}_z$$
$$+ \frac{1}{2m_1R_1^2}\frac{\partial}{\partial\theta}[(\hat{J}_x + i\hat{J}_y) - (\hat{J}_x - i\hat{J}_y)] + V(R_1, R_2, \theta), \quad (2)$$

TABLE I. Calculated geometrical parameters and vibrational fundamental energies of BeH_2.

Basis set	Method	$R_e(a_0)$	$\nu_1(cm^{-1})$	$\nu_2(cm^{-1})$	$\nu_3(cm^{-1})$	Reference
cc-pVQZ	CCSSCF(+F)	2.514				8
	CMRCI(+K)	2.506				8
	MCRCI+Q(+K)	2.506				8
	CASSCF	2.519				8
	CMRCI	2.515				8
	CMRCI+Q	2.515				8
6-311++g(2*d*,*p*)	B3LYP	2.5054				10
	MPW1PW91	2.5169				10
	MP2=(full)	2.5043				10
	CCSD	2.5116				10
aug-cc-pVTZ	B3LYP	2.5037				10
	MPW1PW91	2.5158				10
	MP2=(full)	2.4995				10
	CCSD	2.5192				10
[5*s*3*p*2*d*1*f*]	CCSD(T)	2.5179	1979.6	716.8	2167.2	3
cc-pCVTZ	CCSD(T)		1987.0	705.2	2157.8	9
aug-cc-pV5Z	icMRCI+Q	2.5147	1983.16	710.67	2169.83	Present
aug-cc-pV5Z[a]	icMRCI+Q and ΔV_{core}	2.5067	1991.97	711.77	2178.79	Present
Experiment	Gas phase	2.5065			2178.87	13
Experiment	Matrix			697.9	2159.1	31

[a]The ΔV_{core} energy was calculated at the MR-ACPF/cc-pCV5Z level of theory.

in which m_1 and m_2 are the masses of the two H atoms. The transformation between Radau coordinates (R_1,R_2,θ) and the conventional bond-length/bond-angle coordinates $(R_1^{BeH},R_2^{BeH},\gamma)$ is well documented.[19] Due to the mass disparity between H and Be, the radial Radau coordinates R_1 and R_2 are close to, but not identical with, the corresponding molecular Be–H bonds R_1^{BeH} and R_2^{BeH}. The operators $\hat{J}_x$, $\hat{J}_y$, and $\hat{J}_z$ are the components of the total angular momentum operator $\hat{J}$ in the body-fixed frame. The z axis of the body-fixed frame lies along the R_1 radial Radau vector. The above Hamiltonian contains full vibration-rotation coupling.

A direct-product discrete variable representation (DVR) grid[22] was used in the rovibrational energy level calculation. Each stretching coordinate was represented by a 70-point potential-optimized DVR grid derived from the one-dimensional Hamiltonian, in which two other coordinates were fixed at their equilibrium values, with a 200 equidistant-point sine-DVR grid on the interval $[1.6,5.0]a_0$. Some 80 Gauss-Legendre grid points on the interval [60°–180°] were used for the angular variable. In addition, the potential cutoff was placed at 5.0 eV. The Lanczos algorithm was used to calculate the rovibrational energy levels for $J=0-8$ by recursively diagonalizing the discretized Hamiltonian matrix. Lanczos iterations were found adequate to converge the energies of levels lying within 9000 cm^{-1} of the potential minimum to better than 0.001 cm^{-1}. Spurious eigenvalues were removed using the method detailed in Ref. 23. When eigenfunctions were needed, the Lanczos recursion was repeated to assemble the wave functions of interest.[24]

To obtain the spectroscopic constants of BeH_2 and BeD_2, a least-squares fit was performed to the rotational sublevels for each vibrational level. The appropriate energy level expression for linear triatomic molecules was used,[14]

$$E = G(v_1,v_2^{\ell},v_3) + B[J(J+1)-\ell^2] - D[J(J+1)-\ell^2]^2 + H[J(J+1)-\ell^2]^3 \pm \frac{1}{2}[qJ(J+1) + q_D[J(J+1)]^2 + q_H[J(J+1)]^3], \quad (3)$$

in which B is the inertial rotational constant, D and H the

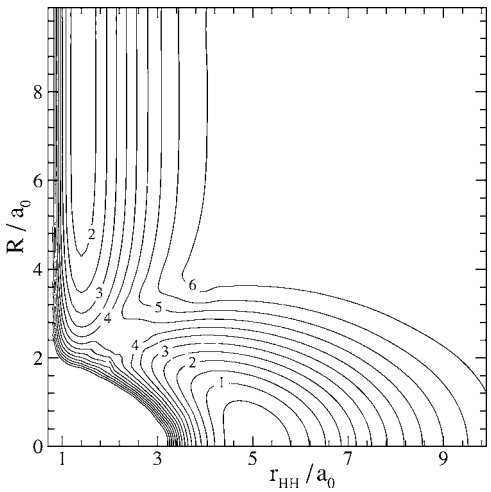

FIG. 3. Contours of the BeH_2 potential energy surface in Jacobi coordinates at the fixed angle $\gamma=90°$. Contours are separated by 0.5 eV, with the zero of energy set at the potential minimum.

TABLE II. Calculated energies (in eV) of BeH_2 dissociation products obtained with different basis sets, expressed relative to the energy at its equilibrium linear geometry.

Method	Transition state	$Be+H_2$[a]	BeH+H[b]	H+Be+H	Source
FCI/5*s*2*p*	4.7974	0.4435	⋯	⋯	Ref. 2
CCSD(T)/A′V5Z	⋯	⋯	⋯	6.4152	Ref. 6
CMRCI/VQZ	4.6633[c]	1.6208			Ref. 8
AV5Z	4.2343[d]	1.6285	4.2112	6.3797	Present
AV5Z+V_{core}	4.2493[e]	1.6628	4.2247	6.4231	Present

[a]Product geometry $r_e^{HH}=1.402a_0$.
[b]Product geometry $r_e^{BeH}=2.5368a_0$.
[c]Transition state geometry $R_1^{BeH}=R_2^{BeH}=2.703a_0$, $\gamma=45.24°$.
[d]Transition state geometry $R_1^{BeH}=R_2^{BeH}=2.8232a_0$, $\gamma=42.08°$.
[e]Transition state geometry $R_1^{BeH}=R_2^{BeH}=2.8221a_0$, $\gamma=42.05°$.

leading centrifugal distortion constants, J is the total angular momentum quantum number (including internal rotation), and $G(v_1,v_2^\ell,v_3)$ is the pure vibrational energy for level (v_1,v_2^ℓ,v_3) relative to the zero-point level at $G(0,0^0,0)$, where ℓ is the vibrational angular momentum quantum number ($\ell=0$, 1, and 2 for Σ, Π, and Δ levels, respectively). For Σ states, the constants $q=q_D=q_H=0$, but they are nonzero for Π and Δ states; the $\pm$ sign refers to the $e(+)$ and $f(-)$ parity. For Δ states, because of the ℓ-type rotational resonances between their $\Delta(e)$ levels and the associated nearby $\Sigma(e)$ states, a 2×2 Hamiltonian matrix was used to describe their levels.[14,25] Those rotational ℓ-type resonances in BeH_2 and BeD_2 are discussed in Ref. 14.

III. RESULTS AND DISCUSSION

A. Potential energy surface

Figures 1 and 2 display contour plots of our potential energy surface for ground-state BeH_2 in internal coordinates $(R_1^{BeH},R_2^{BeH},\gamma)$, the former showing the dependence of the potential energy surface on the two bond lengths with the interbond angle fixed at 180°, while the latter depicts its dependence on one Be–H bond length and the bending angle while the other Be–H bond is fixed near its equilibrium value at $2.506a_0$. The contour levels were determined by three-dimensional spline interpolation over the 6864 symmetry-unique *ab initio* points. The overall minimum clearly lies at the linear geometry, and for our highest level (AV5Z+V_{core}) calculations, corresponds to $R_1^{BeH}=R_2^{BeH}=2.5067a_0$ (1.3265 Å). Table I compares this result with previous theoretical values reported for this species and with experiment; our value is clearly in excellent agreement with the experimental bond length of 1.326 41 Å. A full listing of the 6864 symmetry-unique potential function values defining this surface may be obtained from the authors or from the journal's data archive.[26]

The linear-geometry potential minimum on our surface lies 6.4231 eV (or 148.12 kcal/mol) below the asymptote corresponding to H+Be+H. Taking account of the zero-point energy yields an atomization energy of $D_0=6.0704$ eV (or 139.99 kcal/mol), which is in good agreement with Martin's theoretical estimate of 140.86 kcal mol^{-1}.[6] To illustrate the exit channel for the reaction $BeH_2\rightarrow Be+H_2$, Fig. 3 shows our potential energy surface along a decomposition/insertion pathway perpendicular to the H–H bond, using $Be+H_2$ Jacobi coordinates $(R,r_{HH},\chi=90°)$. This decomposition reaction is clearly endothermic, and our calculations show that BeH_2 is more stable than the separated $Be+H_2$ products by 1.6285 eV (or 37.554 kcal/mol) and 1.6628 eV (38.345 kcal/mol) at the AV5Z and AV5Z+V_{core} levels of theory, respectively (not including the zero-point energy). These values are in reasonably good agreement with the theoretical value of 37.38 kcal/mol reported by Hinze *et al.*[8] This result differs from the situation for the analogous linear molecules MgH_2 and HgH_2, for which the decomposition channels for the reaction $MH_2\rightarrow M+H_2$ (M=Mg,Hg) are exothermic.[27,28] The BeH_2 molecule is also stabilized by a large barrier along this C_{2v} reaction path; the saddle point of the barrier is found to lie at $R_1^{BeH}=R_2^{BeH}=2.8221a_0$ (1.4934 Å) and $\gamma=42.05°$, which is slightly different from the location $R_1^{BeH}=R_2^{BeH}=2.703a_0$ (1.430 Å) and $\gamma=45.24°$ calculated by Hinze *et al.*[8] Our predicted barrier heights for this reaction $BeH_2\rightarrow Be+H_2$ are 4.2355 eV (97.673 kcal/mol) and 4.2493 eV (97.991 kcal mol^{-1}) at the AV5Z and AV5Z+V_{core} levels of theory, respectively; both of these estimates are lower than the value of 4.6633 eV (107.54 kcal/mol) calculated by Hinze *et al.* at the CMRCI/VQZ level.[8]

The other BeH_2 decomposition channel, namely, $BeH_2\rightarrow BeH+H$, is predicted to be strongly endothermic by 4.2112 eV (97.112 kcal/mol) and 4.2247 eV (97.424 kcal/mol) at the AV5Z and AV5Z+V_{core} levels of theory, respectively. The calculated relative energies of various dissociation limits and of the transition state, relative to the triatomic potential minimum, at different levels of theory are summarized in Table II.

B. Interpolation to define the potential energy surface

A question which must always be asked when calculating level energies and molecular properties on a pointwise *ab initio* potential energy surface is the magnitude of the

TABLE III. Root mean square discrepancy (in cm^{-1}) on interpolating for omitted potential function values in the specified range when the independent variable interpolated over was $V(R_i^{BeH})^n$, for $n=0$, 2, and 4.

Range	No. points	$n=0$	$n=2$	$n=4$
All energies	6864	97.93	5.63	73.53
Energies $\leqslant 20\,000$ cm^{-1}	1857	6.60	0.89	3.07

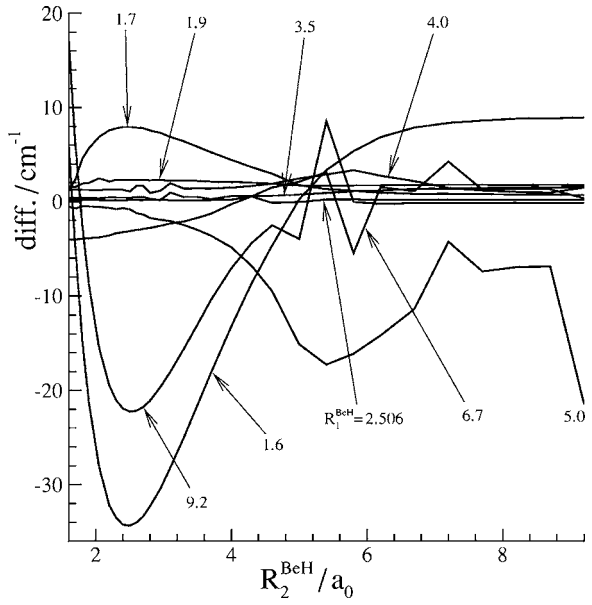

FIG. 4. Errors in interpolated potential function values as function of one Be–H bond length R_2^{BeH}, for selected values of the other, R_1^{BeH}, with the bending angle fixed at the equilibrium value of $\gamma=180°$.

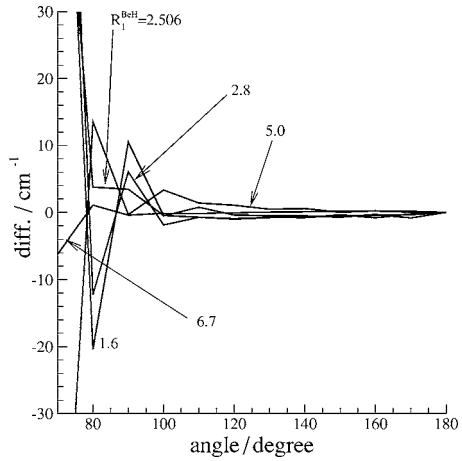

FIG. 5. Errors in interpolated potential function values as functions of the bending angle for various values of one Be–H bond length R_1^{BeH}, with the other fixed at $R_2^{BeH}=2.506a_0$.

"interpolation noise" uncertainty, that is, the degree to which the results obtained depend on the particular method used for interpolating between the grid points. If this interpolation noise is unreasonably large, it usually means that the grid does not contain a sufficiently dense mesh of point in some region(s) of configuration space. The present work examined this question in two ways. One was to omit known potential function values from the grid and examine the magnitudes of the errors in the estimates of their value obtained using different interpolation schemes; the other was to compare calculated values of vibrational energies computed using the different schemes.

The interpolation schemes used in these tests all involved conventional "rectangular" three-dimensional spline interpolation, in which the function value at an intermediate coordinate position is obtained by stepwise one-dimensional spline interpolation along the three internal coordinate axes, R_1^{BeH}, R_2^{BeH}, and γ. In one approach, the quantity interpolated over was the potential function value itself, $V(R_1^{BeH}, R_2^{BeH}, \gamma)$. In the others, interpolation along the bond-stretch axes treated $(R_i^{BeH})^n V$ as the dependent variable, where the power $n=2$ or 4; after such an interpolation is performed, division of the result by $(R_i^{BeH})^n$ yields the desired function value. Experience with diatomic molecules had shown that in the short-range repulsive wall region where the potential function is growing particularly rapidly, use of this scaled ordinate variable yielded much more reliable interpolation results.[29,30]

The first row of Table III shows that when all of our potential function points are considered, a remarkable factor of 17 reduction in the root mean square (rms) interpolation discrepancy is obtained if the interpolation is performed over $(R_i^{BeH})^2 V$ rather than over the potential function itself (the case $n=0$). This is due to the fact that the rapid decrease of the factor $(R_i^{BeH})^2$ with decreasing bond length damps the growth of the ordinate variable in that region, which improves the reliability of the cubic spline interpolation procedure.[29,30] The fact that increasing the power further to $n=4$ causes the rms discrepancy to increase by over an order of magnitude mainly reflects the fact that the lower part of the outer attractive wall of our potential function is also very steep, and this further modification makes the ordinate variable there grow sufficiently rapidly with distance that a cubic spline function may no longer interpolate accurately. The last row of Table III shows the analogous rms discrepancies for the 1857 configurations corresponding to energies within 20 000 cm^{-1} of the potential minimum. Again, $n=2$ interpolation has substantially smaller discrepancies than for the other cases, and for $n=2$, "interpolation noise" errors in the potential energy function are on average less than 1 cm^{-1}. This $n=2$ cubic spline interpolation scheme was therefore used in our final calculations of the spectroscopic properties of BeH_2, BeD_2, and BeHD.

For all cases, the largest contributions to these rms discrepancies occur at geometries far from equilibrium where the grid of potential function values is least dense. This is illustrated by Fig. 4, which shows for $n=2$ interpolation how the potential energy discrepancies at omitted points depend on R_2^{BeH} at various values of R_1^{BeH} for a linear molecular geometry ($\gamma=180°$). When R_1^{BeH} is close to the equilibrium value of 2.5067 Å, the differences are very small for all values of R_2^{BeH}. Similarly, Fig. 5 plots the $(n=2)$ interpolation discrepancies at omitted angular points as a function of the bending angle for various values of one Be–H stretching coordinate (R_1^{BeH}) when the other was fixed near its equilibrium value. It is again clear that interpolation discrepancies are lowest near the potential minimum configuration $(\gamma=180°)$.

Finally, the energies of the 62 lowest pure vibrational levels of BeH_2 calculated using the $n=0$, 2, and 4 interpolation schemes were compared with one another. With the $n=2$ results taken as the reference case, the rms discrepancies for eigenvalues calculated with $n=0$ and 4 were 0.080 and

TABLE IV. Calculated energies (in cm^{-1}) of the lowest 48 pure vibrational levels of BeH_2, BeD_2, and BeHD on the AV5Z+V_{core} potential energy surface. The BeH_2 levels are listed in order of increasing energy; level energies for the heavier isotopologs which do not appear in order of increasing energy are labeled by an asterisk, and the highest-energy level for each is shown in bold font.

(v_1,v_2^{ℓ},v_3)	BeH_2	BeD_2	BeHD
$(0,0^0,0)$	0.00	0.00	0.00
$(0,2^0,0)$	1417.27	1089.19	1262.95
$(1,0^0,0)$	1991.97	1425.24	2106.14*
$(0,0^0,1)$	2178.79[a]	1689.27[b]	1537.76
$(0,4^0,0)$	2831.14	2169.71	2518.58
$(1,2^0,0)$	3406.85	2521.93	3350.67
$(0,2^0,1)$	3570.10	2760.37	2800.20*
$(2,0^0,0)$	3953.43	2836.31	4153.26
$(1,0^0,1)$	4112.25	3083.66	3637.63*
$(0,6^0,0)$	4241.79	3242.83	3767.79*
$(0,0^0,2)$	4323.80[c]	3356.06[d]	3045.66*
$(1,4^0,0)$	4816.82	3607.64	4587.94
$(0,4^0,1)$	4958.01	3822.92	4053.12*
$(2,2^0,0)$	5365.12	3940.48	5378.60
$(1,2^0,1)$	5500.53	4161.92	4882.68*
$(0,8^0,0)$	5649.31	4309.40	5011.15
$(0,2^0,2)$	5690.03	4409.42	4307.18*
$(3,0^0,0)$	5882.98	4233.13*	6143.09
$(2,0^0,1)$	6010.82	4462.83	5676.79*
$(1,0^0,2)$	6206.48	4721.09	5140.27*
$(1,6^0,0)$	6222.27	4684.21*	5818.85*
$(0,6^0,1)$	6342.71	4878.27	5297.97*
$(0,0^0,3)$	6434.32[e]	5000.51	4523.64*
$(2,4^0,0)$	6770.26	5031.11	6596.74
$(1,4^0,1)$	6883.85	5229.33	6118.25*
$(0,10^0,0)$	7052.97	5370.09	6249.07
$(0,4^0,2)$	7053.72	5454.37	5556.71*
$(3,2^0,0)$	7290.24	5344.80*	7345.78
$(2,2^0,1)$	7394.70	5548.13	6903.78*
$(1,2^0,2)$	7570.43	5781.49	6385.35*
$(1,8^0,0)$	7623.49	5752.89*	7043.97*
$(0,8^0,1)$	7724.25	5927.23	6535.63*
$(0,2^0,3)$	7775.95	6036.46	5783.93*
$(4,0^0,0)$	7777.96	5615.70*	8077.63
$(3,0^0,1)$	7872.07	5826.60*	7656.33*
$(2,0^0,2)$	8055.50	6070.23	7172.95*
$(2,6^0,0)$	8169.39	6110.76	7808.57*
$(1,6^0,1)$	8262.63	6287.76	7348.38*
$(1,0^0,3)$	8269.71	6337.49	6613.81*
$(0,6^0,2)$	8412.82	6492.33	6796.37*
$(0,12^0,0)$	8454.94	6425.40*	7481.81*
$(0,0^0,4)$	8510.43	6622.86	5971.80*
$(3,4^0,0)$	8688.87	6440.01*	**8546.49**
$(2,4^0,1)$	8771.87	6619.95	8121.37*
$(1,4^0,2)$	8929.94	6831.14	7618.45*
$(1,10^0,0)$	9020.64	6814.59*	8262.91*
$(0,10^0,1$	9102.67	6970.45	7766.75*
$(0,4^0,3)$	**9114.32**	**7064.19**	7029.34*
$(0,2^0,4)$			7230.58*
$(0,0^0,5)$			7390.41*
$(1,2^0,3)$			7858.45*
$(0,8^0,2)$			8027.48*
$(1,0^0,4)$			8058.02*
$(0,6^0,3)$			8263.80*
$(2,2^0,2)$			8401.02*
$(0,4^0,4)$			8471.09*

[a]Experimental value of 2178.87 (Ref. 13).
[b]Experimental value of 1689.68 (Ref. 13).
[c]Experimental value of 4323.78 (Ref. 13).
[d]Experimental value of 3356.74 (Ref. 13).
[e]Experimental value of 6434.11 (Ref. 13).

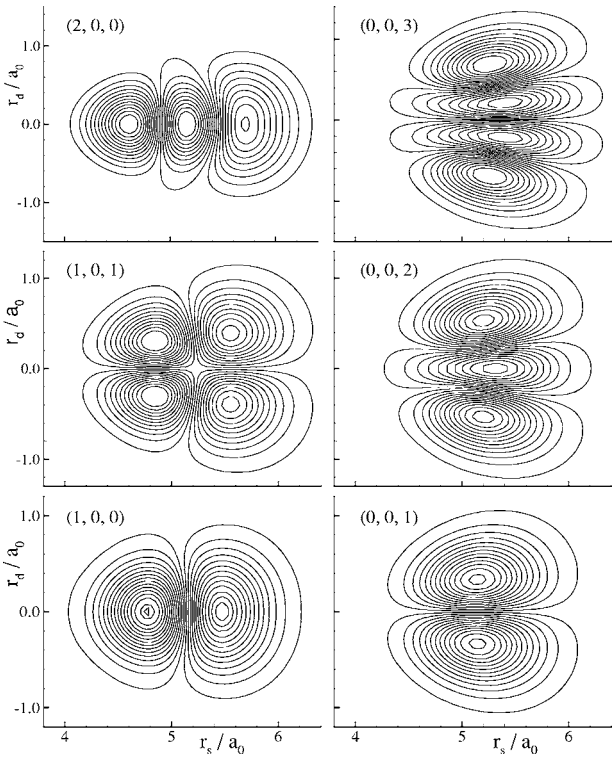

FIG. 6. Contour plots for six vibrational eigenfunctions of BeH_2: $(v_1,v_2,v_3)=(1,0,0)$, (0,0,1) (1,0,1), (0,0,2), (2,0,0), and (0,0,3) in sum $r_s=(R_1+R_2)$ and difference $r_d=(R_1-R_2)$ Radau coordinates, shown for $\gamma=180°$.

0.038 cm^{-1}, respectively. In view of the relative merits of the various interpolation schemes shown by Table III, it therefore seems clear that the absolute interpolation noise uncertainties associated with our $n=2$ rovibrational eigenvalues are of order 0.01 cm^{-1}.

C. Vibration-rotation energy levels and spectroscopic constants

The vibrational zero-point levels of BeH_2, BeD_2, and BeHD are found to lie 2844.33 cm^{-1} (or 0.3527 eV), 2130.21 cm^{-1} (or 0.2641 eV), and 2493.00 cm^{-1} (or 0.3091 eV), respectively, above the triatomic potential minimum. One can see from Table II that this zero-point level for BeH_2 is lower than the dissociation asymptotes to yield $Be+H_2$ (1.6628 eV) or BeH+H (4.2247 eV), lower than the atomization energy of 6.4231 eV at AV5Z+V_{core} level, and significantly below the large barrier (4.2493 eV) to the $Be+H_2$ asymptote mentioned above. Thus, the vibrational ground state and the low-lying excited vibrational states are truly stable.

Table IV lists the pure vibrational ($J=0$) level energies of BeH_2, BeD_2, and BeHD calculated from the AV5Z+V_{core} potential energy surface. The first 48 levels of BeH_2 are listed in order of increasing energy, while corresponding levels of BeD_2 and BeHD which do not appear in order of increasing energy are labeled with an asterisk. The highest energy level for each isotopolog is shown in bold font, and the additional levels of BeHD lying below those highest levels are included at the end of the list. For BeH_2 and BeD_2, the three quantum numbers labeling each vibrational level (v_1,v_2,v_3) represent the symmetric-stretch, bend, and antisymmetric-stretch modes, respectively. For BeH_2, our calculated fundamental frequency for the antisymmetric-stretch vibration and its first and second overtones, 2178.79, 4323.80, and 6434.32 cm^{-1}, respectively, are in very good agreement with the experimental gas phase values of Shayesteh *et al.*:[13] 2178.87, 4323.78, and 6434.11 cm^{-1}, respectively. Similarly, our values for the analogous fundamental and first overtone asymmetric-stretch energies for BeD_2,

TABLE V. Spectroscopic constants (in cm^{-1}) for BeH_2 calculated from our AV5Z+V_{core} potential energy surface, and their difference (calc.−obs.) with the corresponding experimental values (Ref. 14).

	G_v-ZPE		B		10^4D		10^9H		10^2q		10^6q_D		$10^{10}q_H$	
Levels	Calc.	Diff.	Calc.	Diff.	Calc.	Diff.	Calc.	Diff.	Calc.	Diff.	Calc.	Diff.	Calc.	Diff.
$(0,0^0,0)$	0.00	0.00	4.7023	0.0009	1.0528	0.0028	3.00	0.29						
$(0,0^0,1)$	2178.79	−0.08	4.6333	0.0011	1.0360	0.0029	2.93	0.30						
$(0,0^0,2)$	4323.80	0.02	4.5656	0.0014	1.0196	0.0026	2.87	0.30						
$(0,0^0,3)$	6434.32	0.21	4.4989	0.0017	1.0040	0.0055	2.82	0.82						
$(1,0^0,0)$	[a]		4.6456	0.0012	1.0442	0.0018	2.95	0.17						
$(1,0^0,1)$	a+2120.28	0.12	4.5755	0.0014	1.0289	0.0029	3.36	0.70						
$(0,1^1,0)$	[b]		4.7130	0.0010	1.0958	0.0050	3.58	0.54	−9.148	−0.008	8.33	0.21	−10.8	−2.8
$(0,1^1,1)$	b+2165.8	−0.01	4.6440	0.0012	1.0795	0.0048	3.51	0.52	−9.107	−0.008	8.25	0.22	−11.1	−3.1
$(0,1^1,2)$	b+4298.26	0.15	4.5762	0.0014	1.0634	0.0041	3.46	0.51	−9.069	−0.008	8.17	0.19	−10.9	−2.8
$(1,1^1,0)$	[c]		4.6558	0.0013	1.0853	0.0034	3.52	0.43	−9.010	0.012	8.07	−0.57	−10.8	2.6
$(1,1^1,1)$	c+2106.97	0.18	4.5857	0.0015	1.0698	0.0029	3.43	0.37	−8.961	0.013	7.96	−0.63	−9.1	4.7
$(0,2^0,0)$	[d]		4.7247	0.0010	1.1442	0.0046	4.28	0.58						
$(0,2^2,0)$	d+10.61	0.05	4.7225	0.0010	1.1378	0.0041	4.11	0.53	−9.203	−0.011	8.63	0.26	−11.2	−3.0
$(0,2^0,1)$	d+2152.83	0.02	4.6557	0.0013	1.1284	0.0052	4.06	0.50						
$(0,2^2,1)$	d+2163.34	0.09	4.6534	0.0012	1.1221	0.0038	4.29	0.74	−9.158	−0.010	8.55	0.22	−12.0	−3.6
$(0,2^0,2)$	d+4272.76	0.21	4.5878	0.0015	1.1127	0.0023	4.00	0.02						
$(0,2^2,2)$	d+4283.18	0.30	4.5856	0.0015	1.1062	0.0050	4.07	0.74	−9.117	−0.011	8.50	0.19	−13.8	−3.0

[a]1991.07 cm^{-1}.
[b]711.07 cm^{-1}.
[c]2702.78 cm^{-1}.
[d]1417.27 cm^{-1}.

TABLE VI. Spectroscopic constants (in cm^{-1}) for BeD_2 calculated from our AV5Z+V_{core} potential energy surface, and their difference (calc.−obs.) with the corresponding experimental values (Ref. 14).

	G_v-ZPE		B		10^5D		$10^{10}H$		10^2q		10^6q_D		$10^{10}q_H$	
Levels	Calc.	Diff.	Calc.	Diff.	Calc.	Diff.	Calc.	Diff.	Calc.	Diff.	Calc.	Diff.	Calc.	Diff.
$(0,0^0,0)$	0.00	0.00	2.360 34	−0.0006	2.624 780	0.0042	3.75	0.54						
$(0,0^0,1)$	1689.27	−0.40	2.329 70	−0.0006	2.574 601	−0.0154	3.54	−1.64						
$(0,0^0,2)$	3356.06	−0.68	2.299 50	−0.0004	2.525 827	0.0093	3.50	0.62						
$(0,1^1,0)$	[a]		2.367 20	−0.0006	2.720 969	0.0276	4.35	2.77	−2.985	0.033	1.31	−0.59	−1.05	3.66
$(0,1^1,1)$	a+1680.20	−0.36	2.336 55	−0.0005	2.670 471	−0.0006	4.40	−0.79	−2.995	0.035	1.31	−0.71	−0.75	5.46
$(0,2^0,0)$	[b]		2.374 21	−0.0007	2.822 479	0.0182								
$(0,2^2,0)$	b+10.14	0.03	2.373 70	−0.0005	2.810 835	0.0539			−2.988	−0.009	1.36	0.16		
$(0,2^0,1)$	b+1671.17	−0.33	2.343 56	−0.0006	2.772 469	0.0142								
$(0,2^2,1)$	b+1681.26	−0.29	2.343 05	−0.0003	2.758 704	0.0688			−2.996	−0.010	1.36	0.20		

[a]548.36 cm^{-1}.
[b]1089.19 cm^{-1}.

1689.27 and 3356.06 cm^{-1}, respectively, agree very well with the experimental gas phase values[13] of 1689.68 and 3356.74 cm^{-1}, respectively. For the case of BeHD, the vibrational quantum numbers (v_1,v_2,v_3) represent the Be–H stretch, the bend, and the Be–D stretch modes, respectively. No experimental infrared spectra for HBeD have been reported to date.

Contour plots of the wave functions for a number of levels of BeH_2 are shown in Fig. 6, plotted versus the symmetric and antisymmetric combinations of Radau coordinates $r_s=R_1+R_2$ and $r_d=R_1-R_2$. The nodal structures of these wave functions are quite clear; wave function plots of this type were used to make the vibrational assignments for the levels listed in Table IV.

Tables V and VI present detailed comparisons of our calculated results on the AV5Z+V_{core} potential energy surface with the experimental spectroscopic constants for all of the emission bands of BeH_2 and BeD_2 reported by Shayesteh *et al.*[13,14] To facilitate direct comparisons with the experimental band origins, our calculated energies for the lower levels of vibrational transitions which are not directly connected to the ground state are shown as footnotes, rather than in the tables themselves. The calculated constants are clearly in very good agreement with the observed values. For BeH_2, rms discrepancies are roughly 0.028% for the B rotational constants, 0.36% for the D constants, and 15% for the H centrifugal distortion constants, while the rms discrepancy with the 11 observed band origins was 0.15(±0.09) cm^{-1}.

TABLE VII. Spectroscopic constants (in cm^{-1}) for levels of BeHD calculated from our AV5Z+V_{core} potential energy surface.

Levels	G_v-ZPE	B	10^5D	10^9H	10^2q	10^6q_D	$10^{10}q_H$
$(0,0^0,0)$	0.00	3.2324	5.2446	0.95			
$(0,0^0,1)$	1537.76	3.1948	5.2112	0.97			
$(0,0^0,2)$	3045.66	3.1571	5.1685	1.04			
$(0,0^0,3)$	4523.64	3.1193	5.1078	1.23			
$(1,0^0,0)$	2106.14	3.1943	5.1523	0.83			
$(2,0^0,0)$	4153.26	3.1568	5.0297	0.88			
$(3,0^0,0)$	6143.09	3.1187	4.9183	0.93			
$(1,0^0,1)$	3637.63	3.1548	5.2179	0.51			
$(1,0^0,2)$	5140.27	3.1065	5.3620	⋯			
$(2,0^0,1)$	5676.79	3.1191	5.0336	0.71			
$(0,1^1,0)$	635.55	3.2402	5.4226	1.10	−4.860	3.124	−2.41
$(0,1^1,1)$	2173.56	3.2031	5.3597	1.19	−4.755	3.051	−2.60
$(0,1^1,2)$	3681.62	3.1668	5.2268	⋯	−4.537	3.536	⋯
$(1,1^1,0)$	2732.42	3.2017	5.3329	1.00	−4.961	2.929	−3.28
$(2,1^1,0)$	4769.89	3.1642	5.2099	1.02	−4.963	2.959	−3.12
$(1,1^1,1)$	4264.69	3.1621	5.3747	0.83	−5.072	2.250	−4.04
$(0,2^0,0)$	1262.95	3.2483	5.6362	1.23			
$(0,2^2,0)$	1275.16	3.2471	5.5912	1.25	−4.867	3.297	−2.82
$(1,2^0,0)$	3350.67	3.2098	5.5456	1.15			
$(1,2^2,0)$	3362.64	3.2085	5.5021	1.14	−4.954	3.130	−3.32
$(2,2^0,0)$	5378.60	3.1723	5.4228	1.16			
$(2,2^2,0)$	5390.33	3.1710	5.3793	1.17	−4.958	3.130	−3.11
$(0,2^0,1)$	2800.20	3.2114	5.5641	1.34			
$(0,2^2,1)$	2813.07	3.2104	5.5069	1.35	−4.765	3.218	−2.62
$(0,2^0,2)$	4307.18	3.1757	5.4446	1.46			
$(0,2^2,2)$	4320.90	3.1750	5.3472	1.76	−4.571	3.479	−1.95

The analogous differences for BeD_2 are generally somewhat larger: the rms discrepancies for the rotational constants were 0.023%, 1.2%, and 46% for B, D, and H, respectively, and that for the band origins was 0.46(±0.19) cm^{-1}. However, this increase is to be expected because the rotational energy interval sampled by the $J=0-8$ range of calculated levels used to determine these parameters was a factor of 2 smaller than for BeH_2.

Our calculations also allow us to generate values of the g_{22} constant associated with the ℓ-dependent term in the vibrational level energy expression for a symmetric triatomic molecule. For $\Pi(\ell=2)$ and $\Sigma(\ell=0)$ vibrational levels

$$g_{22}=[G(v_1,v_2^2,v_3)-G(v_1,v_2^0,v_3)]/4. \quad (4)$$

The results in Tables V and VI give us values of $g_{22}=2.65$, 2.63, and 2.60_5 cm^{-1} for the (0,2,0), (0,2,1), and (0,2,2) levels of BeH_2, and 2.53_5 and 2.52 cm^{-1} for the (0,2,0) and (0,2,1) levels of BeD_2. These are within 0.01–0.02 of the experimental values of Shayesteh *et al.*[14]

Finally, Table VII presents our predicted energies and rotational constants for 26 vibrational levels of BeHD, arranged to illustrate the dependence of the various properties on vibrational quantum number for a given mode. Note that the form of our vibrational energy expression Eq. (3) means that for levels with $\ell>0$, the $J=\ell$ level does not have zero rotational energy.

IV. CONCLUSIONS

We report an *ab initio* potential energy surface for the ground electronic state of BeH_2 consisting of 6864 symmetry-unique points obtained at the icMRCI+Q level with a large basis set and including core-electron correlation contributions. Eigenvalues of low-lying levels of BeH_2, BeD_2, and HBeD calculated using the iterative Lanczos method converged to better than 0.001 cm^{-1} were used to generate the energies and rotational constants of a number of vibrational levels of the three isotopologs, BeH_2, BeD_2, and BeHD. These results are in excellent agreement with the gas phase spectroscopic results of Shayesteh *et al.*:[13,14] our band origins had rms discrepancies of 0.15(±0.09) and 0.46(±0.19) cm^{-1} and our inertial rotational constants had rms relative discrepancies of 0.028% and 0.023% for BeH_2 and BeD_2, respectively. These band origin discrepancies are two orders of magnitude smaller than those in the best previous *ab initio* treatment of this system.[3] This demonstrates the high quality of our potential energy surface and indicates that our predictions of the properties of unobserved levels should be quite reliable. Tests using various interpolation schemes showed that the "interpolation noise" uncertainties in the calculated eigenvalues are $\lesssim 0.01$ cm^{-1}. Listings of our *ab initio* potential function values and of the $J=0-8$ level energies used to determine the rotational constants presented in Tables V–VII may be obtained from the authors, or from the AIP's Electronic Physics Auxiliary Publication Service (EPAPS).[26]

ACKNOWLEDGMENTS

We are pleased to acknowledge helpful discussions with Professor P. F. Bernath and Dr. A. Shayesteh, and we thank Dr. Shayesteh for his assistance with some of the fits used to determine our spectroscopic constants. We are also grateful to Professor Kirk Peterson for providing us with his new Be atom basis set prior to publication. This research was supported by the Natural Science and Engineering Research Council of Canada.

[1] G. D. Purvis III and R. J. Bartlett, J. Chem. Phys. **76**, 1910 (1982).
[2] G. D. Purvis, R. Sheoard, F. B. Brown, and R. J. Bartlett, Int. J. Quantum Chem. **23**, 825 (1983).
[3] J. M. L. Martin and T. J. Lee, Chem. Phys. Lett. **200**, 502 (1992).
[4] P. G. Szalay and R. J. Bartlett, J. Chem. Phys. **103**, 3600 (1996).
[5] L. Füsti-Molnár and P. G. Szalay, J. Phys. Chem. **100**, 6288 (1996).
[6] J. M. L. Martin, Chem. Phys. Lett. **273**, 98 (1997).
[7] N. Ben Amor and D. Maynau, Chem. Phys. Lett. **286**, 211 (1998).
[8] J. Hinze, O. Friedrick, and A. Sundermann, Mol. Phys. **96**, 711 (1999).
[9] T. Hrenar, H.-J. Werner, and G. Rauhut, Phys. Chem. Chem. Phys. **7**, 3123 (2005).
[10] R. A. Klein and M. A. Zottola, Chem. Phys. Lett. **419**, 254 (2006).
[11] See, for example, S. R. Radel and M. H. Navidi, *Chemistry* (West, St. Paul, MN,1990), p. 390.
[12] P. F. Bernath, A. Shayesteh, K. Tereszchuk, and R. Colin, Science **297**, 1323 (2002).
[13] A. Shayesteh, K. Tereszchuk, P. F. Bernath, and R. Colin, J. Chem. Phys. **118**, 3622 (2003).
[14] A. Shayesteh and P. F. Bernath, J. Chem. Phys. **124**, 156101 (2006).
[15] H. J. Werner, P. J. Knowles, R. D. Amos *et al.*, MOLPRO, a package of *ab initio* programs.
[16] S. R. Langhoff and E. R. Davidson, Int. J. Quantum Chem. **8**, 61 (1974).
[17] D. E. Woon, K. A. Peterson, and T. H. Dunning Jr., J. Chem. Phys. (submitted).
[18] R. J. Gdanitz and R. Ahlrichs, Chem. Phys. Lett. **143**, 413 (1988).
[19] B. R. Johnson and W. P. Reinhardt, J. Chem. Phys. **85**, 4538 (1986).
[20] S. E. Choi and J. C. Light, J. Chem. Phys. **92**, 2129 (1990).
[21] B. T. Sutcliffe and J. Tennyson, Int. J. Quantum Chem. **39**, 183 (1991).
[22] J. C. Light, I. P. Hamilton, and J. V. Lill, J. Chem. Phys. **82**, 1400 (1985).
[23] R. Chen and H. Guo, J. Chem. Phys. **111**, 9944 (1999).
[24] J. K. Collum and R. A. Willoughby, *Lanczos Algorithms for Large Symmetric Eigenvalue Computations* (Birkhauser, Boston, 1985).
[25] D. Papousek and M. R. Aliev, *Molecular Vibrational-Rotational Spectra* (Elsevier, Amsterdam, 1982).
[26] See EPAPS Document No. E-JCPSA6-125-303625 for an ASCII file containing a complete listing of the 6864 energies defining our recommended AV5Z+V_{core} potential energy surface for BeH_2. This document can be reached via a direct link in the online article's HTML reference section or via the EPAPS homepage (http://www.aip.org/pubservs/epaps.html).
[27] H. Li, D. Q. Xie, and H. Guo, J. Chem. Phys. **121**, 4156 (2004).
[28] H. Li, D. Q. Xie, and H. Guo, J. Chem. Phys. **122**, 144314 (2005).
[29] J. D. Poll and G. Karl, Can. J. Phys. **44**, 1467 (1966).
[30] R. J. Le Roy and R. B. Bernstein, J. Chem. Phys. **49**, 4312 (1968).
[31] T. Tague, Jr. and L. Andrews, J. Am. Chem. Soc. **115**, 12111 (1993).